GEOPHYSICAL RESEARCH LETTERS, VOL. 23, NO. 9, PAGES 957-960, MAY 1, 1996

Antarctic ice sheet melting in the Southeast Pacific

Stanley S. Jacobs and Hartmut H. Hellmer
Lamont-Doherty Earth Observatory of Columbia University, Palisades, NY

Adrian Jenkins
British Antarctic Survey, Cambridge, UK

Abstract. The first oceanographic measurements across a deep channel beneath the calving front of Pine Island Glacier reveal a sub-ice circulation driven by basal melting of 10-12 m yr^{-1}. A salt box model described here gives a melt rate similar to that of ice balance and numerical models, 5-50 times higher than averages for the George VI and Ross Ice Shelves. Melting is fueled by relatively warm Circumpolar Deep Water that floods the deep floor of the Amundsen and Bellingshausen Sea continental shelves, reaching the deep draft of this floating glacier. A revised melt rate for ice shelves in the Southeast Pacific sector raises circumpolar ice shelf melting to 756 Gt yr^{-1}. Given prior estimates of surface accumulation and iceberg calving, this suggests that the Antarctic Ice Sheet is currently losing mass to the ocean.

Background

In early 1994, an oceanographic survey of the southern Amundsen and Bellingshausen Seas (Figure 1) entered Pine Island Bay and reached the calving front of Pine Island Glacier (PIG; Figure 2). The floating part of PIG is 70-90 km long, moves at velocities up to 2.6 km yr^{-1}, and drains a catchment basin of ~ 200,000 km^2 [*Crabtree and Doake* 1982; *Lucchitta et al.* 1995]. We evaluate the mass balance of PIG in Jenkins et al. [subm.], showing that about half the mass flux across the grounding line is calved as icebergs at the ice front. This implies that the floating PIG is either rapidly growing in size or has a basal melt rate of 12 ±3 m yr^{-1}. A simple box model consistent with oceanographic measurements made near the ice front supports that high melt rate, which has implications for mass balance of the Antarctic Ice Sheet.

Circulation and Melting

Vertical temperature and salinity profiles to the sea floor near PIG show a homogeneous thermohaline layer at depths >800 m (Figure 3). With temperatures above +1°C and dissolved oxygen below 4.4 ml l^{-1}, this layer is clearly derived from lower Circumpolar Deep Water (CDW) north of the continental shelf. Temperature and salinity decrease toward the sea surface in steps and inversions, some resembling features modelled or recorded near glacial ice floating in salt water [*Huppert and Turner* 1980; *Jacobs et al.* 1981; *Jenkins* 1993]. On Station 92 in particular, the temperature-salinity ratio (dT/dS = 2.8) is close to that expected for seawater modified by melting ice [*Gade* 1979; *Potter et al.* 1988; *Nost and Foldvik* 1994]. That work shows the salinity of melt-laden water

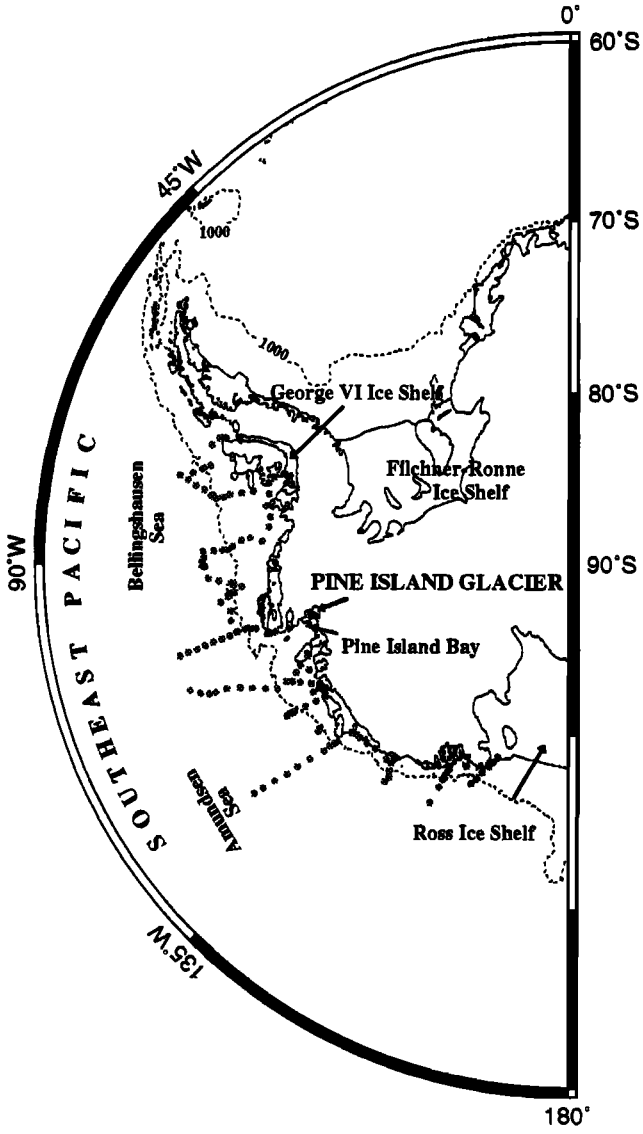

Figure 1. Pine Island Glacier (PIG) and other West Antarctic features in relation to the SE Pacific Ocean. The continental shelf break is near the 1000 m bathymetric contour (dashed line). The dots show stations occupied from the *Nathaniel B. Palmer* in February-March 1994.

Paper number 96GL00723
0094-8534/96/96GL-00723$05.00

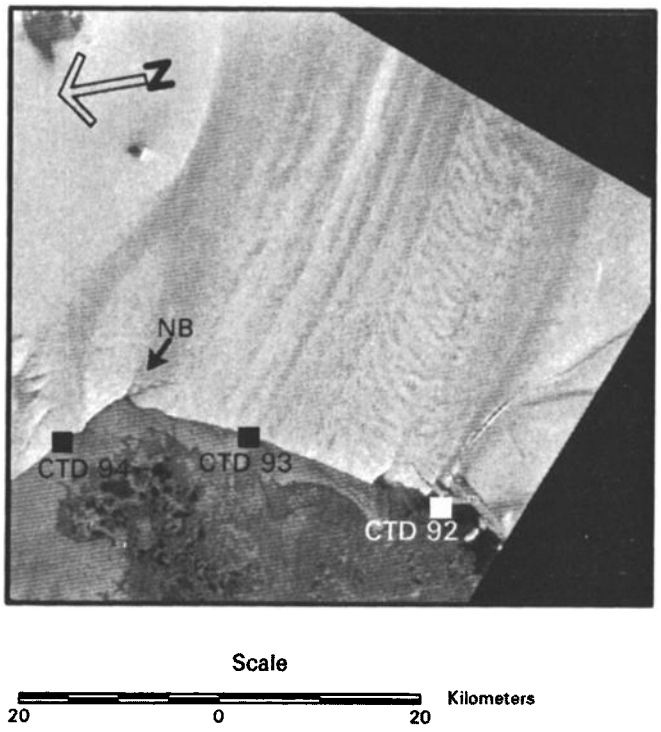

Figure 2. A March 15, 1994, ERS-1 SAR (synthetic aperture radar) satellite image of the western end of PIG. The northern boundary of the calving front is shown by the NB arrow, and the southern boundary is near CTD 92, located at 75°03.6S, 101°50.8W. The PIG floats above a 70-90 km-long cavity with a draft ranging from <340 m at the ice front to >1200 m near the grounding line [*Crabtree and Doake* 1982; *Jenkins et al.* subm.].

depends upon the thermohaline properties of source water and the temperature difference between the two. Other stations in Pine Island Bay show a similar bottom layer, but have more typical salt-stabilized inverse thermoclines and higher temperature/salinity ratios trending toward freezing at salinities of ~34.1. The latter probably indicate late-winter surface conditions in the region.

The warmest, most saline water occurs near the sea floor on stations 92 and 93 (Figure 3) and presumably fills the deeply-cut channel below 800 m in Figure 4. From that depth up to ~450 m, seawater salinity (density) is lower on the south side of the cavity opening, consistent with a Coriolis-deflected outflow, as observed moving at 10-25 cm s^{-1} from beneath the northwest front of George VI Ice Shelf [*Potter and Paren* 1985]. Although geostrophic equilibrium is doubtful near boundaries and large vertical motions, a rough transport estimate can be obtained from dynamic height differences between CTD profiles 92 and 93. These stations are more widely spaced than the local Rossby radius, but encompass >70% of the cavity opening beneath PIG. Over the 340-800 m-depth range, a transport of 0.172 Sv (1 Sv = 10^6 m^3 s^{-1}) corresponds to a mean outflow velocity of 2.0 cm s^{-1}. In this melt-driven circulation, balance would be achieved by an equivalent inflow over the smaller area below 800 m, corresponding to a velocity of 4.3 cm s^{-1}. The outflow velocity compares favorably with the mean of 1.9 cm s^{-1} from four current meters moored for up to a year in the main outflow from beneath the Ross Ice Shelf [*Jacobs et al.* 1992]. We would expect higher velocities and a concentrated outflow above 600 m in the water column near Station 92 (Figure 4).

A melt rate of 10.5 m yr^{-1} is obtained over a basal area of 3.0 x 10^3 km^2, using the 0.172 Sv transport, an ice density of 917 kg m^{-3} and a salinity decrease of 0.183 between inflow (average salinity >800 m) and outflow (average salinity, 340-800 m) on Station 92. Some of this freshening could come from other melting ice in the region, or from beneath the grounded ice sheet. However, the lower-salinity outflow will likely extend several kilometers to the south of Station 92, upwell very near the ice front and emerge from shallower basal crevasses (Figure 4). Net cooling of 0.51°C between inflow (average temperature >800 m) and outflow (average temperature from 340-800 m) on Station 92 implies a heat loss of 3.6 x 10^{11} W. That is sufficient to support heat flux into the ice over a vertical temperature gradient of ~23°C, melt a little more than 10.5 m yr^{-1}, and warm the meltwater by 3°C.

The ocean circulation beneath PIG can be modelled like that of the larger ice shelves *[e.g., Hellmer and Jacobs* 1995], using an ice draft profile from Crabtree and Doake [1982]. The unknown sea floor profile between the ice front and grounding line can be tuned to produce an outflow with temperature and salinity close to the values

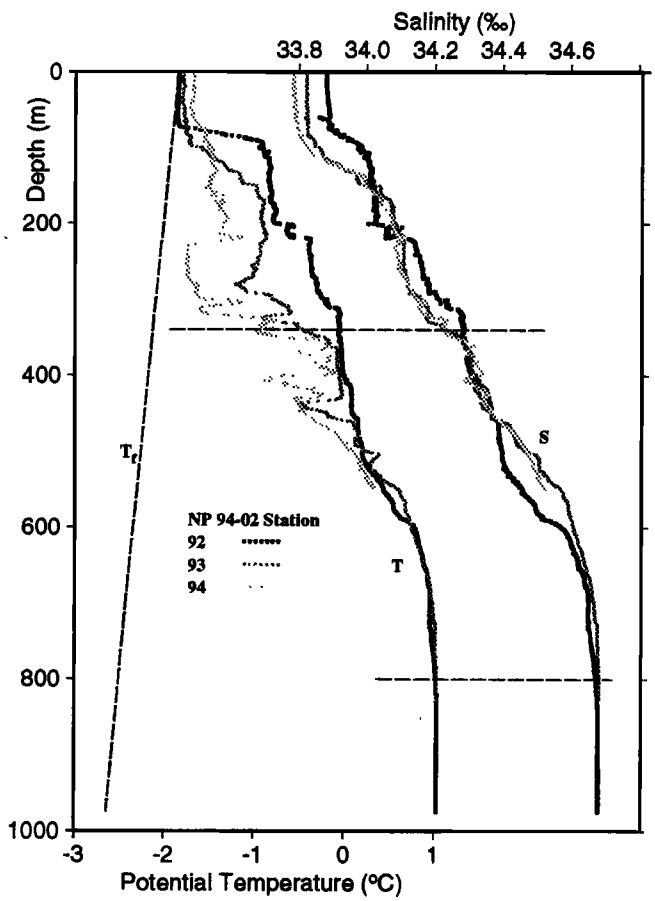

Figure 3. Potential temperature and salinity vs. depth on stations 92-94, taken near the PIG (Figure 2) on March 14, 1994. Horizontal dashed lines show the 340 m draft of PIG (Figure 4) and the 800 m division between deep inflow and shallower outflow. Water below 800 m is >3°C warmer than the in-situ freezing temperature (T_f).

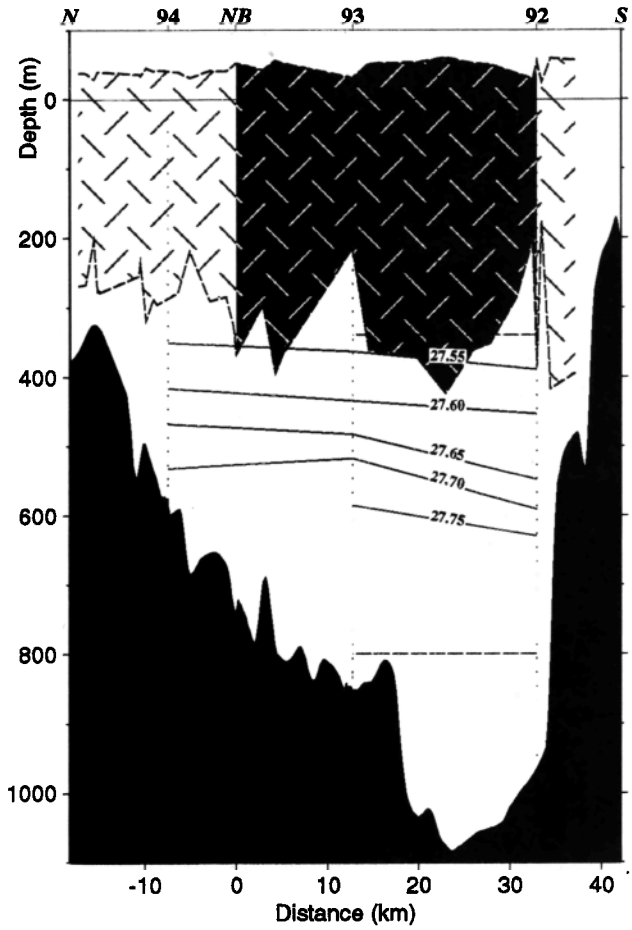

Figure 4. Section across the PIG calving front (hatched dark shading between NB and 92), showing the cavity opening, and the bathymetry from sonic depth recordings. The mean draft of 340 m is based upon ice elevations measured from the ship, and an ice density of 900 kg m^{-3}. The ocean density field (27.55 - 27.75 isopycnals) is from the thermohaline data in Figure 3.

observed on station 92. Hellmer et al. [in prep.] show this results in a simple bottom profile, flow reversal near 800 m, and average melting of 11.6 m yr^{-1}. Three nearly independent methods thus point to an average basal melt rate of 12 ±3 m yr^{-1}.

Mass Balance Implication

Up to the present time, the highest melt rate calculated for floating continental ice attached to Antarctica has been the 1.7-2.1 m yr^{-1} average reported for George VI Ice Shelf [*Potter and Paren* 1985; *Potter et al.* 1988]. The reason for the much higher melt PIG rate is that its draft reaches well below 800 m into the >1°C CDW. In combination with a steeper basal slope [*Crabtree and Doake* 1982], that allows a faster-rising and warmer meltwater plume. CDW has long been known to intrude onto the continental shelf directly west of the Antarctic Peninsula [*Arctowski and Thoulet* 1901; *Talbot,* 1988; *Hofmann et al.* 1995]. The deep continental shelf stations in Figure 1 reveal that CDW intrusions occur throughout the southeast Pacific. This water is >2°C warmer than at most other locations on the Antarctic shelf. Ocean circulations similar to those beneath George VI and PIG are thus likely beneath the other small glaciers and ice shelves on the Amundsen and Bellingshausen Sea continental shelf. Assuming that shallow-draft ice shelves are more common in this sector, their average melt rate may be closer to that of George VI.

Jacobs et al. [1992] summarized in-situ melting of the Antarctic ice shelves from a variety of observations, modelling and glaciological calculations. For the undifferentiated ice shelves, net melting of 0.3 m yr^{-1} was assumed, based upon determinations of the basal mass balance within 100 km of the calving front of the Ross Ice Shelf. That rate now appears too low for the SE Pacific, where floating glaciers and ice shelves cover ~125,000 km^2, an average of areas in Barkov [1985] and Drewry et al. [1982]. Replacing our earlier assumption for that area with a 10 m yr^{-1} rate for PIG and a 2 m yr^{-1} George VI-rate for the remainder raises circumpolar ice shelf melting to 756 Gt yr^{-1} (Table). This may still be conservative, as some past attrition estimates have been restricted to outflows with in-situ temperatures below the sea surface freezing point. The PIG results indicate that melt-laden outflows can be as much as 2°C above freezing.

Large uncertainties accompany all budget terms relevant to Antarctic Ice Sheet mass balance. The ice shelves comprise a very small portion of the ice sheet volume, but account for most all of its attrition via iceberg calving and basal melting. Our revised estimate for ice shelf melting is higher than any previously reported [*Drewry and Morris* 1992], moving the annual budget more firmly into the red (Figure 5). If estimates of surface accumulation and iceberg calving are not too low or high, respectively, the negative balance in this figure indicates that the Antarctic Ice Sheet is currently losing mass to the ocean. An unexplained 0.45 mm yr^{-1} of recent global sea level rise [*Warrick and Oerlemans* 1990] would be resolved if only 25% of the apparent imbalance in Figure 5 came from the grounded ice.

Table. Melting rates of Antarctic ice shelves

Feature	Area $10^3 km^2$	Rate cm yr^{-1}	Melt Gt yr^{-1}
Ice shelf bases:			
Filchner-Ronne	400	55	202
Ross	400	22	81
Amery	39	65	23
George VI	25	190	44
Pine Island Glacier	3	1000	28
Other SE Pacific	122	200	224
<100 km from coast	503	30	138
Ice shelf fronts:	3.5	500	16
		Total melting:	756

Filchner-Ronne and Ross Ice Shelf areas areas are >100 km from their ice fronts. Area <100 km from coast is the difference between total ice shelf area [*Drewry et al.* 1982, *Shabtaie and Bentley* 1987] and itemized features. Amery Ice Shelf is near 71°E. 1 Gt = 10^{12}kg. Ice density = 917 kg m^{-3}. From Jacobs et al. [1992], who estimated melt errors at ± 50%.

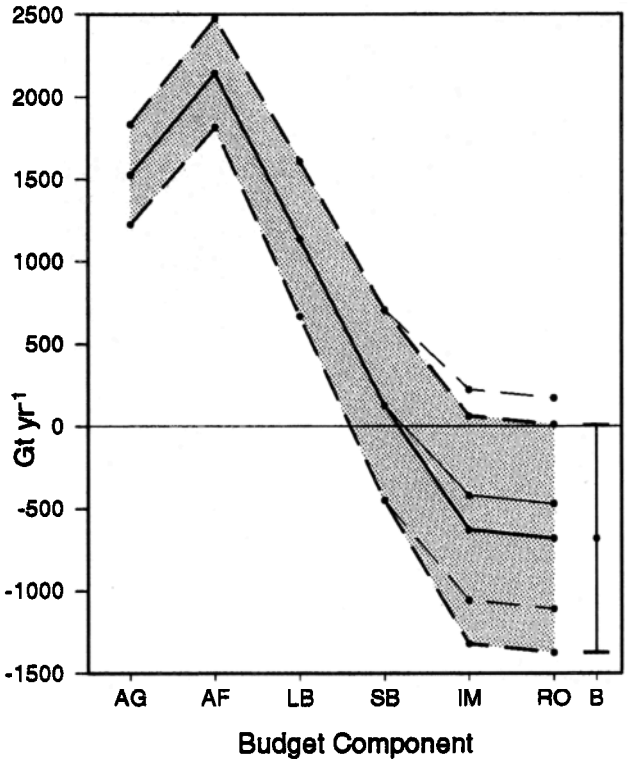

Figure 5. Cumulative growth and attrition components of the Antarctic Ice Sheet annual budget, with error estimates in the shaded band, from Jacobs et al. [1992]. Accumulation is divided between grounded and floating ice (AG and AF), calving between large and small icebergs (LB and SB) and melting between ice shelf and runoff (IM and RO). Increased ice shelf melting (IM) in the Southeast Pacific results in a more negative balance than shown previously by the lighter dashed lines.

Acknowledgments. We thank C. Giulivi, R. Guerrero, H. Keys, S. O'Hara, S. Peng and D. Vaughan for data acquisition, processing, and assistance with figures. W. Smethie and anonymous reviewers made helpful comments on the manuscript. This work is supported by the National Science Foundation and the Department of Energy. Lamont-Doherty Earth Observatory contribution 5470.

References

Arctowski, H. and J. Thoulet, Oceanographie, Rapports Scientifiques, Voyage du S.Y. Belgica, 1897-1899, J. E. Buschmann, Anvers, 23 pp., 1901.

Barkov, N. I., Ice Shelves of Antarctica, Transl. of 1971 Russian edition, Amerind, NY, 262 pp., 1985.

Crabtree, R. D. and C. S. M. Doake, Pine Island Glacier and its drainage basin: Results from radio-echo sounding, *Ann. Glaciol., 3,* 65-70, 1982.

Drewry, D. J., S. R. Jordan and E. Jankowski, Measured properties of the Antarctic ice sheet: Surface configuration, ice thickness, volume and bedrock characteristics, *Ann. Glaciol., 3,* 83-91, 1982.

Drewry, D. J. and E. M. Morris, Response of large ice sheets to climatic change, *Phil. Trans. Roy. Soc. London, Ser. B, 338(1285),* 235-242, 1992.

Gade, H. G., Melting of ice in sea water: A primitive model with application to the Antarctic ice shelf and icebergs, *J. Phys. Ocean., 9(1),* 189-198, 1979.

Hellmer, H. H. and S. S. Jacobs, Seasonal circulation under the eastern Ross Ice Shelf, Antarctica, *J. Geophys. Res., 100(C6),* 10,873-10,885, 1995.

Hofmann, E., J. M. Klinck, C. M. Lascara and D. A. Smith, Water mass distribution and circulation west of the Antarctic Peninsula, in Foundations for Ecological Research west of the Antarctic Peninsula, edited by R. Ross et al., Ant. Res. Ser., AGU, in press, 1995.

Huppert, H. E. and J. S. Turner, Ice blocks melting into a salinity gradient, *J. Fluid Mech.,* 100, 367-384, 1980.

Jacobs, S. S., H. E. Huppert, G. Holdsworth and D. J. Drewry, Thermohaline steps induced by melting of the Erebus Glacier Tongue, *J. Geophys. Res., 86,* 6547-6555, 1981.

Jacobs, S. S., H. H. Hellmer, C. S. M. Doake, A. Jenkins & R. M. Frolich, Melting of ice shelves and the mass balance of Antarctica, *J. Glaciol., 38(130),* 375-387, 1992.

Jenkins, A., Melting of continental ice in the ocean and its impact on surface and bottom waters, in Ice in the Climate System, edited by W. R. Peltier, pp. 217-235, Springer-Verlag, Berlin, 1993.

Lucchitta, B. K., C. E. Rosanova and K. F. Mullins, Velocities of Pine Island Glacier, West Antarctica, from ERS-1 SAR images, *Ann. Glaciol., 21,* 277-283, 1995.

Nost, O. A., and A. Foldvik, A model of ice shelf-ocean interaction with application to the Filchner-Ronne and Ross Ice Shelves, *J. Geophys. Res., 99(C7),* 14,243-14,254, 1994.

Potter, J. R. and J. G. Paren, Interaction between ice shelf and ocean in George VI Sound, Antarctica, in Oceanology of the Antarctic Continental Shelf, Ant. Res. Ser., Vol. 43, edited by S. Jacobs, 35-38, AGU, Washington, 1985.

Potter, J. R., M. H. Talbot and J. G. Paren, Oceanic regimes at the ice fronts of George VI Sound, Antarctic Peninsula, *Cont. Shelf Res., 8(4),* 347-362, 1988.

Shabtaie, S. and C. R. Bentley, West Antarctic ice streams draining into the Ross Ice Shelf: Configuration and mass balance, *J. Geophys. Res., 92(B2),* 1311-1336, 1987.

Talbot, M. H., Oceanic environment of George VI Ice Shelf, Antarctic Peninsula, *Ann. Glaciol., 11,* 161-164, 1988.

Warrick, R. and J. Oerlemans, Sea level rise, in Climate Change: The IPCC Scientific Assessment, edited by J. Houghton et al., 257-281, Cambridge Univ. Press, 1990.

S. Jacobs and H. Hellmer, Lamont-Doherty Earth Observatory, Palisades, NY 10964. (e-mail: sjacobs or hhellmer@lamont.columbia.edu)

A. Jenkins, British Antarctic Survey, Cambridge CB3 0ET, UK. (e-mail: ajen@pcmail.nerc-bas.ac.uk)

(Received October 11, 1995; revised January 5, 1996; accepted February 2, 1996)